RESEARCH ARTICLE   OPEN ACCESS

Solar System Based Static Compensator For Power Quality Enhancement Using T-Connected Transformer

P.Suresh[1] and G.Vijayakumar[2]

[1] Assistant Professor, Department of Electrical and Electronics Engineering, Dr.Nagarathinam's College of Engineering, Namakkal, Tamil Nadu, India
[2] Associate Professor, Department of Electrical and Electronics Engineering, Muthayammal Engineering College, Rasipuram, Namakkal, Tamil Nadu, India

Abstract:

This paper deals with a model of Photovoltaic interface with boost converter fed four-leg VSC (Voltage Source converter) with T connected transformer for power quality enhancement. A synchronous reference frame theory is planned for three-phase four-wire Static Compensator which includes converter, inductor and capacitor. The proposed Static Compensator provides harmonic reduction, reactive power compensation and neutral current compensation at the point of common coupling (PCC). The Photovoltaic array interface with boost converter is used to build up the voltage to match the DC link constraint of the four-leg VSC. The major benefit of this proposed approach is that, it will provide regular compensation for the complete day and grid interface converter can effectively be utilize to transfer of active power produce from the renewable resource. The T connected transformer is responsible for isolation to the VSC and passageway to the zero sequence fundamental harmonics current. To obtain the reference current in order to generate the firing pulse to the SAF, the whole arrangement is planned, established and validated by using MATLAB–SIMULINK environment.

Keywords **- Three-phase four-wire, Static Compensator, T - Connected transformer, Boost converter, Harmonic reduction, current compensation**

1. Introduction

In current scenario researchers have interest on renewable energy based power quality enhancement in the power system because of extensive use of non-linear electronic loads [1, 2]. The usage of fossil fuels causes global warming whose objectionable effects and also insufficient on globe. For a viable world the usage of fossil fuels must be decreased, in fact ended. As an alternative, the usage of renewable energy sources must be increased because it does not cause greenhouse effect in contrary to the fossil fuels. It is sensible that

a solar system can provide an uninterrupted supply of energy due to cyclical variations. The

Photovoltaic arrangement has the ability to acquaintance it in sequence to offer the essential dc voltage. The generated power from the Photovoltaic arrangement requires power condition equipment before connecting it to the dc link [3-5]. Thus the DC-DC boost converter is used to build up the voltage level.

The three-phase four-wire (3P4W) distribution system employed to distribute the electric power neither single-phase nor three-phase loads in residential, commercial and industrial buildings. For single phase loads supply is provide between one of the phase conductors to neutral wires and these loads are not balanced, as a result net current flowing through the neutral conductor and initiate harmonics.

It's not only the source for neutral current and also the usage of nonlinear loads such as Power electronic converters; Adjustable speed drives, uninterruptable power supplies etc. are the liable factor for the power quality issues.

The power quality at the distribution system is governed by various standards such as IEEE-519 standard [6]. The investigation to power quality problems are reported in the literature and are known by the universal name of custom power devices (CPD) [7]. These custom power devices include the DSTATCOM (distribution static compensator), DVR (dynamic voltage restorer), SAF (Static Compensator) and UPQC (unified power quality conditioner). The SAF is a parallel linked device which focusses the power quality problems.

Some of the topologies of Static Compensator interface with three-phase four-wire system for the mitigation of neutral current and power quality compensation. Four-leg voltage source converter (VSC), three single-phase VSCs, three-leg VSC with split capacitors, three-leg VSC with zigzag transformer, and three-leg VSC with neutral terminal at the positive or negative of dc bus [8-11]. The voltage regulation in the distribution feeder is improved by installing a shunt compensator. There are various schemes stated in the literature for control of SAF such as synchronous reference frame theory, IcosΦ algorithm, instantaneous reactive power theory, hysteresis bang-bang compensation, etc. [12-14]. The synchronous reference frame theory is used for the control of the proposed Static Compensator.

In this paper, a new methodology of SAF grid interfaced T-connected transformer is proposed for the three-phase four wire distribution system [15-18]. T-connected transformer offers current cancellation at neutral conductor and mitigates the harmonics, the SAF interfaced boost converter compensates the source harmonic neutral current, load reactive power, and balances load. The IGBT based VSC is self-supported with a dc bus capacitor and is controlled for the required compensation of the load current. The Static Compensator is designed and simulated using MATLAB software with its Simulink and power system block set (PSB) toolboxes for source harmonic neutral current compensation, THD (Total Harmonic Distortion) reduction and reactive power compensation at nonlinear loads.

2. System configuration and design

The boost converter interfaced four-leg VSC with T connected transformer is coupled at point of common coupling (PCC) with nonlinear load is shown in Fig. 1. The VSC has an inductors, insulated-gate bipolar transistors (IGBTs) and dc capacitors. The dc bus voltage of VSC generally depends on the instantaneous energy available to the Static Compensator [19]. The dc bus voltage is designed as,

$$V_{dc} = \frac{2\sqrt{2}\,V_{LL}}{\sqrt{3}\,m} \qquad (1)$$

Where V_{LL} is the ac line voltage of SAF and m is the modulation index, consider V_{LL} of 415 V and modulation index is 1. Then, V_{dc} is obtained as 678V and is preferred as 700V.
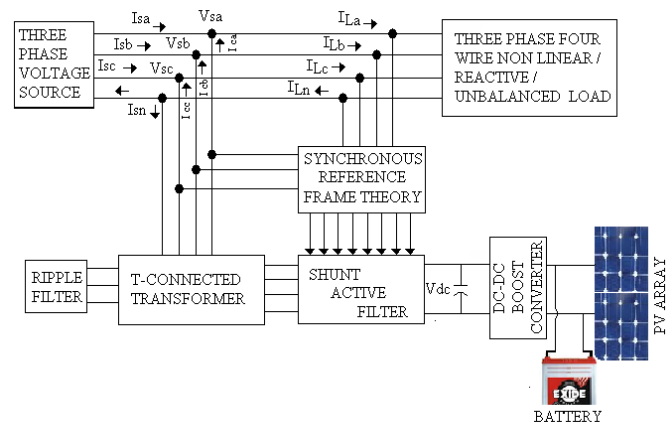

Fig. 1. Block diagram of proposed renewable based four-leg VSC with

T-connected transformer.

The dc capacitor (C_{dc}) of VSC designed with related to the instantaneous energy present in the SAF during transient conditions [19]. The dc capacitor is designed as,

$$\frac{1}{2}C_{dc}\left[\left(V^2_{dc}\right) - \left(V^2_{dc1}\right)\right] = 3V(aI)t \qquad (2)$$

Where Vdc1 is the least voltage of dc link capacitor and Vdc is the reference voltage of dc link capacitor, V is the phase voltage, a is the overloading factor, I is the phase current and t is time required for dc link capacitor recovery. During transient condition Consider, a 1.5% of in dc link capacitor decreased, Vdc = 700 V, Vdc1 = 690 V, V = 239.60 V, a = 1.2, I = 28.76 A, t = 350 µs, the designed value of C_{dc} is 1228 µF and is chosen as 1500 µF.

The value of AC inductor of VSC depends on, dc bus voltage (V_{dc}), the current ripple (I_{cr}) and switching frequency fs and L_f is given as [19]

$$L_f = \frac{\sqrt{3} m V_{dc} I_{cr}}{12\, a f_s}$$

(3)

Consider, peak to peak current ripple $I_{cr\ p-p}$ is 5%, dc bus voltage V_{dc} is 700 V, m is modulation index is 1, a is the overloading factor 1.2 and switching frequency fs is 10 KHz the designed value of L_f to be 0.421mH

A low-pass filter is regulated at half the switching frequency to filter the high frequency noise at the PCC. A low impedance of 8.1 Ω is taken into the consideration for a frequency of 5 kHz, the ripple filter has series resistance (R_f) of 5 Ω is included in series with the capacitor (C_f) as 5 µF. A. The impedance is 637 Ω at 50Hz frequency, which is adequately large and the ripple filter has negligible fundamental current.
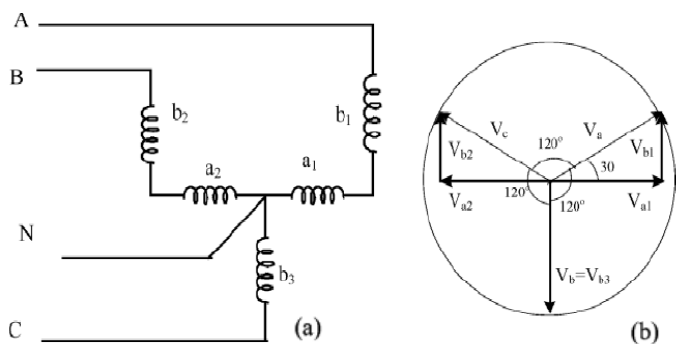
2.1 Design of the T-connected Transformer

Fig. 2. (a): T-connected transformer (b) Phasor diagram

A three-phase four-wire grid interfaced T-connected transformer has two single phase transformer in T-configuration, connection and phasor diagram as shown in Fig. 2a and b . The T-connected transformer provides neutral current cancellation and zero-sequence fundamental harmonic current when it's connected in parallel to PCC. The zero-sequence fundamental current is split into three currents and flow through the windings of the transformer during unbalanced load conditions. The current rating of the windings is decided by the required neutral current compensation [15-18]. Turn's ratio of the transformer windings decides the voltage range across each winding. Consider V_a is the resultant voltage and V_{a1} & V_{b1} are the voltages across each winding then

$$V_{a1} = K_1 V_a \qquad (4)$$
$$V_{a2} = K_2 V_a \qquad (5)$$

Where K_1 and K_2 are the winding fractions in the phases.

For the instant $|V_a| = |V_b| = V$ then the voltages across V_{a1} is equal to $V_a \cos 30°$ and V_{b1} is equal to $V_a \sin 30°$. From equation (4) and (5), the winding fractions $K_1 = 0.866$ and $K_2 = 0.5$. Consider the line voltage is $V_{ca} = 415$ V, then

$$V_a = V_b = V_c = 415 \sqrt{3} = 239.60 \text{ V} \qquad (6)$$
$$V_{a1} = 207.49 \text{ V}, V_{b1} = 119.80 \text{ V} \qquad (7)$$

From the equation, ratings of the transformer are chosen 5kVA, 240V/120V/120V and 5kVA, 208V/208V.

3. System modeling and control

A simple PV cell is essentially an ideal current source in parallel with an ideal diode. The current source represents the current generated by the PV cell due to the photons received by it. PV cells have nonlinear characteristics which vary with radiation intensity and temperature. PV cells produce sufficient power if connected in series. The single-diode

equivalent circuit of a PV cell as show in Fig. 3. The circuit is composed of a current source, a diode, series, and parallel resistance. Solar irradiation level will change due to the weather fluctuations for different cities in Tamilnadu [20] as shown in Table 1. From the table, it is observed that the Solar irradiation may vary between 5.03 - 5.16 Kwh/m^2/day.
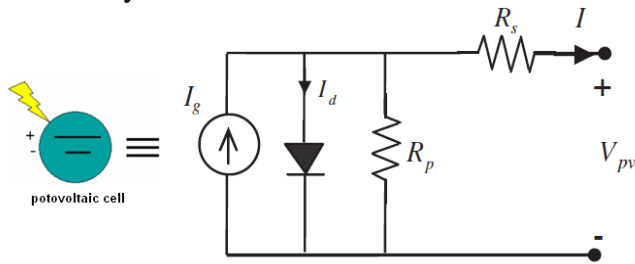

Fig. 3. Single diode equivalent circuit of a real PV cell

Table 1
Solar irradiation for different cities in Tamilnadu Kwh/m^2/day onto horizontal surface(January 2016–December 2016).

City/Month	Jan	Feb	Mar	Apr	May	Jun	July	Aug	Sep	Oct	Nov	Dec	Avg
Chennai	4.9	5.8	6.6	6.6	6	5.1	4.6	4.7	4.9	4.4	4	4.2	5.16
Madurai	4.6	5.4	6.1	5.6	5.6	5.1	4.9	5.1	5.3	4.6	4.1	4.1	5.03
Salem	4.8	5.8	6.4	6.1	5.9	5.1	4.7	4.9	5.2	4.5	4.1	4.3	5.13

Table 2
Parameters of CANADIAN SOLAR CS5P-220M solar panel.

Parameters	Symbol	Typical Value
Nominal Power	P_{max}	220 W
Open Circuit Voltage	V_{oc}	58.8 V
Short Circuit Current	I_{sc}	5.01 A
Temp. Coefficient of Power	k_t	0.45%/K
Temp. Coefficient of Voltage	k_v	0.206V/K
Maximum Power Voltage	V_{mpp}	47 Volts
Maximum Power Current	I_{mpp}	4.68 Amps
Number of Cells	-	96 (8 x 12)
Power per unit of area	-	12.0W/ft^2 (129.4W/m^2)

To represent the Photovoltaic part in MATLAB–SIMULINK, Table 2 shows the CANADIAN SOLAR CS5P-220M datasheet, parameters are obtained at temperature of 25 ^{0}C and solar irradiance of 1000 W/m2. The Photovoltaic components obtain a 47 V voltage and also propose more energy than conventional solar cells [21, 22]. Fig. 4 shows The I–V characteristics of Photovoltaic component at constant temperature of 25^{0}C with variable solar irradiance. The Photovoltaic representation is developed using essential equations

of photovoltaic cells as well as the effects of temperature and solar irradiation [23, 24]. The diode and load current equations are given as,

$$I_d = I_0 \left(e^{\left(\frac{q(V_{pv} + I R_s)}{M_s K T_a}\right)} - 1 \right) \qquad (8)$$

$$I_{pv}(V_{pv}) = I_g - I_d - \left(\frac{V_{pv} + I_{pv} R_s}{R_p}\right) \qquad (9)$$

The highest photovoltaic voltage is obtained under open circuit situation, when $I_{PV} = 0$ with negligible resistance is given as,

$$V_{pv} = \frac{AKT}{Q} \log_n\left(\frac{I_g}{I_d} + 1\right) \qquad (10)$$

Where A is curve fitting constant, k is the Boltzmann constant $(1.381X10^{-23}$ J/K), T is the junction temperature in kelvin (K). I_g is the generated current in photovoltaic module (A) under short circuit condition, I_d is the current shunted through the intrinsic diode, V_{pv} is the Terminal voltage of the cell, R_S ans R_P are Series, shunt Resistance computed from I-V characteristics.
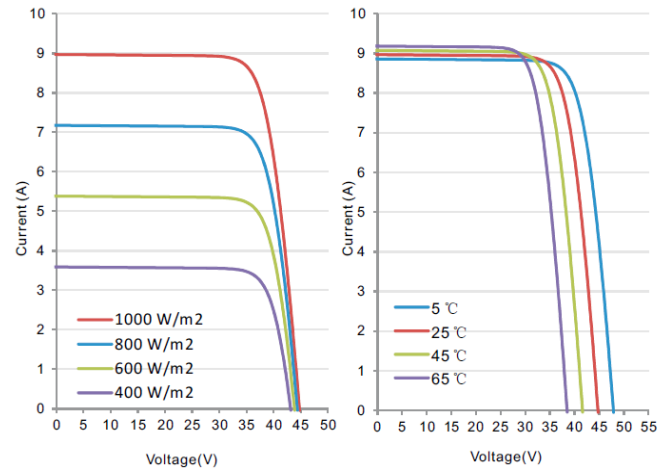

Fig. 4. I-V characteristics CANADIAN SOLAR CS5P-220M solar panel.

Based on the fluctuation in the solar irradiation the proposed methodology has split into three operations. First one, during bright illumination; the photovoltaic arrangement can directly link to the boost converter to increase the voltage and match the dc link voltage. In this case the

battery is not charge. Second one, during excess power, the output voltage of the photovoltaic arrangement drive the boost converter coupled SAF for compensating the source current. In this case the battery is charging. Third one, during dark illumination, the photovoltaic output is absent and the battery has only provision for providing compensation.
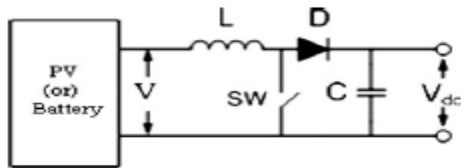

Fig. 5. Schematic diagram of photovoltaic or battery operated boost converter.

The photovoltaic arrangement or battery operated boost converter is shown in Fig. 5. To step up the input voltage to obtain a desired output voltage. The circuit operation is divided into two modes. In mode 1, when the switch is in on condition the input current supplies energy to the inductor for a period T_{on}. Similarly in mode 2, when the switch is off, the inductor voltage adds to the source voltage and current is forced to flow through diode D and the load for a period T_{off}. The PV or battery voltage of 47 V is fed to the boost converter and the output voltage of the boost converter of 676 V is obtained to maintain the dc link voltage of the four-leg voltage source converter. In order to step-up the voltage, a switching frequency of 25 kHz is considered and the inductor value of 0.0191 mH is calculated [25, 26]. The capacitor C of 1500 µF is chosen as per Eq. (2). The output voltage V_{out} is greater than the input Voltage V_{in} and the output equation is shown in the following equation.

$$\frac{V_{out}}{V_{in}} = \frac{1}{1-D} \; where \; V_{out} = V_{dc}, \; V_{in} = V \; and \; D = \frac{T_{on}}{T_{on} + T_{off}} \quad (11)$$

Where V is the PV or battery voltage, D the duty cycle, T_{on} the on time, and T_{off} the off time.

4. Control of SAF

The control scheme block diagram is shown in Fig. 6. Several control methodologies are available to generate reference current for three-phase four-wire system of SAF, synchronous reference frame theory (SRFT), IcosΦ algorithm, instantaneous reactive power theory, hysteresis bang-bang compensation, etc. [12-14]. The SRFT is used in this research for the control of SAF
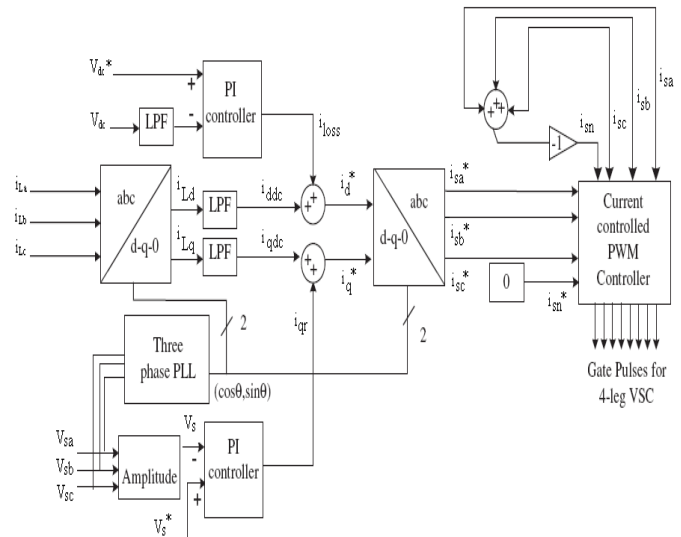

Fig. 6. Control algorithm of four-leg VSC based SAF in three phase four wire system.

The load currents (i_{La}, i_{Lb}, i_{Lc}), the PCC voltages (V_{Sa}, V_{Sb}, V_{Sc}), and dc bus voltage (V_{dc}) of SAF are sensed as feedback signals. The load currents from the a–b–c frame are first converted to the α–β–0 frame and then to the d–q–0 frame using the Park's transformation as in eqn. (12

$$\begin{bmatrix} i_{Lq} \\ i_{Ld} \\ i_{L0} \end{bmatrix} = \frac{2}{3} \begin{bmatrix} \cos\theta & \cos(\theta - \frac{2\pi}{3}) & \cos(\theta + \frac{2\pi}{3}) \\ \sin\theta & \sin(\theta - \frac{2\pi}{3}) & \cos(\theta + \frac{2\pi}{3}) \\ \frac{1}{2} & \frac{1}{2} & \frac{1}{2} \end{bmatrix} \begin{bmatrix} i_{La} \\ i_{Lb} \\ i_{Lc} \end{bmatrix} \quad (12)$$

Where cos θ and sin θ are obtained using a three-phase phase-locked loop (PLL). A PLL signal is obtained from terminal voltages for generation of fundamental unit vectors for conversion of sensed currents to the d–q–o reference frame [27, 28]. The

SRF controller extracts dc quantities by a low-pass filter, and hence, the non-dc quantities are separated from the reference signal. The d-axis and q-axis currents consist of fundamental and harmonic components as

$$i_{Ld} = i_{d\,dc} + i_{d\,ac} \qquad (13)$$
$$i_{Lq} = i_{q\,dc} + i_{q\,ac} \qquad (14)$$

The control strategy for reactive power compensation consider that the source must deliver the mean value of the direct-axis component of the load current along with the active power component current for maintaining the dc bus and meeting the losses (i_{loss}) in SAF. The output of the first proportional-integral (PI) controller at the dc bus voltage of SAF is considered as the current (i_{loss}) for meeting its losses

$$i_{loss(n)} = i_{loss(n-1)} + K_{pq}\big(V_{de(n)} - V_{de(n-1)}\big) + K_{iq}V_{de(n)} \qquad (15)$$

Where $V_{de(n)}$ is the error between the reference voltage ($V_{dc}*$) and sensed dc voltages ($V_{dc(n)}$) at the nth sampling instant. K_{pq} and K_{iq} are the proportional and integral gains of the dc bus voltage PI controller. The reference source current is therefore

$$i_d{}^* = i_{d\,dc} + i_{loss} \qquad (16)$$

The reference source current must be in phase with the voltage at the PCC but with no zero-sequence component. It is therefore obtained by the following reverse Park's transformation with i_d* as in (12) and i_q* and i_0* as zero

$$\begin{bmatrix} i_{sa}{}^* \\ i_{sb}{}^* \\ i_{sc}{}^* \end{bmatrix} = \begin{bmatrix} \cos\theta & \sin\theta & 1 \\ \cos\left(\theta - \dfrac{2\pi}{3}\right) & \sin\left(\theta - \dfrac{2\pi}{3}\right) & 1 \\ \cos\left(\theta + \dfrac{2\pi}{3}\right) & \sin\left(\theta + \dfrac{2\pi}{3}\right) & 1 \end{bmatrix} \begin{bmatrix} i_d{}^* \\ i_q{}^* \\ i_0{}^* \end{bmatrix} \qquad (17)$$

Likewise, the amplitude of ac terminal voltage (V_S) at the PCC is controlled to its reference voltage (V_S*) using the PI controller. The output of PI controller is considered as the reactive component of current (i_{qr}) for zero voltage regulation of ac voltage at PCC. The amplitude of ac voltage (V_S) at PCC is calculated from the ac voltages (V_{sa}, V_{sb}, V_{sc}) as

$$V_s = \left(\frac{2}{3}\right)^{1/2} \left(V_{sa}{}^2 + V_{sb}{}^2 + V_{sc}{}^2\right)^{1/2} \qquad (18)$$

Then, a PI controller is used to regulate this voltage to a reference value as

$$i_{qr(n)} = i_{qr(n-1)} + K_{pq}\big(V_{te(n)} - V_{te(n-1)}\big) + K_{iq}V_{te(n)} \qquad (19)$$

Where $V_{te(n)} = V_S* - V_{S(n)}$ denotes the error between reference (V_S*) and actual ($V_{S(n)}$) terminal voltage amplitudes at the nth sampling instant. K_{pq} and K_{iq} are the proportional and integral gains of the dc bus voltage PI controller. The reference source quadrature-axis current is

$$i_q{}^* = i_{q\,dc} + i_{loss} \qquad (20)$$

The reference source current is obtained by reverse Park's transformation using with i_d* as in (equation no) and i_q* as in (equation no) and i_0* as zero. The gains of the controllers are obtained using the Ziegler-Nichols step response technique [29-31]. A step input of amplitude (U) is applied and the output response of the dc bus voltage is obtained for the open-loop system. The maximum gradient (G) and the point at which the line of maximum gradient crosses the time axis (T) are computed. The gains of the controller are computed using the following equations:

$$K_p = \left|\frac{1.2U}{GT}\right| \qquad (21)$$
$$K_i = \left|\frac{0.6U}{GT^2}\right| \qquad (22)$$

In a current controller, the sensed and reference supply currents are compared and a proportional controller is used for amplifying current error in each phase before comparing with a

triangular carrier signal to generate the gating signals for six IGBT switches of VSC of SAF. The gating signals for the fourth leg of VSC of the SAF are obtained from the error signal by comparing sensed (i_{sn}) and reference (i_{sn}^*) neutral currents. The reference and estimated signals of neutral current are obtained as,

$$i_{sn}^* = 0 \tag{23}$$

$$i_{sn} = -(i_{sa} + i_{sb} + i_{sc}) \tag{24}$$

Two PI controllers are used for the purpose of control of dc bus voltage of SAF and ac current at PCC. The compensation current should lead or lag by 90 degree from the voltage. The SAF draws a lagging current to reduce the line-voltage amplitude, when the load injects capacitive reactive power, when the load is an inductive; the SAF operates as a capacitor. Along with reactive current control, the control of SAF consists of the following control functions: harmonic elimination, load balancing and neutral current compensation.

5. Result and discussion

The boost converter fed four-leg VSC with the T connected transformer based SAF in a three-phase four-wire system which is modeled and simulated by using the MATLAB with its SIMULINK environment and PSB toolboxes. The source consists of three phase ac voltages with neutral and non-linear loads are connected at PCC. The SAF is coupled in parallel to the system through interfacing inductances. The electrical power system under nonlinear load condition for source voltage and source current without compensation is shown in Fig. 7a and Fig. 7b. The source current harmonic spectrum without compensation is shown in Fig. 7c with the terminal current THD as 20.80%. At 0.1 s, the load is changed to two phase load and also the load currents are absence between 0.2 s and 0.25 s. These loads are applied again at 0.25 s respectively. The neutral current without the compensation is shown in Fig. 7d.

The source current is still sinusoidal even though the load changes occur is shown in Fig. 8a

with the terminal current THD of 1.48% is shown in Fig. 8b. It is observed from the waveform that the harmonic current is compensated and source current is made sinusoidal as stipulated by IEEE 519 – standard and the neutral current after compensation is shown in Fig. 8c.the source voltage and current are in phase as shown in Fig. 8d.The terminal voltage is maintained to the reference voltage by adjusting the reactive power injection is shown in Fig. 9a at 0.2 s the SAF is connected to the grid. It is also observed that the dc bus voltage of SAF is maintained at the reference value under all disturbances is shown in Fig. 9b.The electrical power system data used for simulation is given in Appendix A. The parameter of the photovoltaic system is given in Table 2.
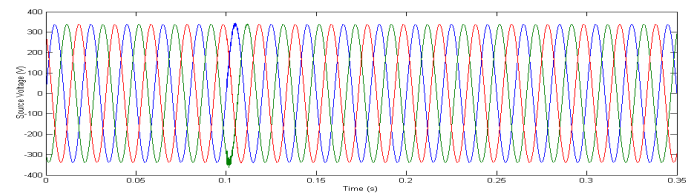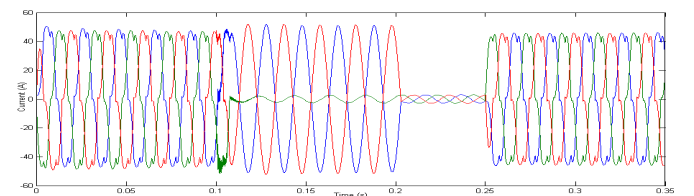

Fig. 7a. Source voltage.

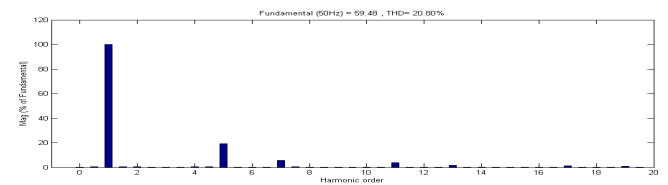**Fig. 7b**. Source current without compensation.

Fig. 7c. Performance of phase A source current with its spectrum without compensation.
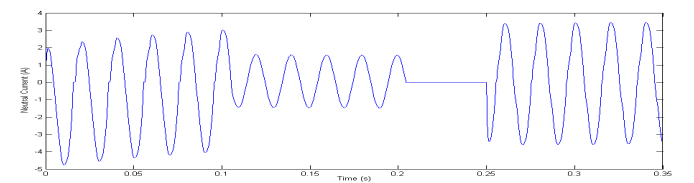

Fig. 7d. Neutral current without compensation.
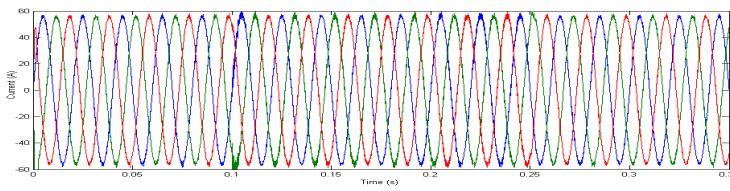
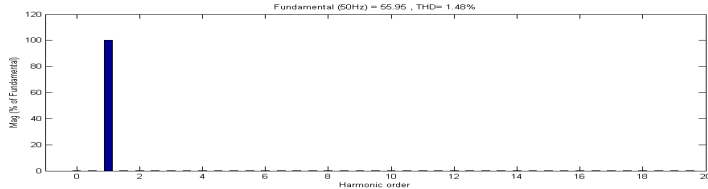**Fig. 8a**. Source current after compensation.

Fig. 8b. Performance of phase A source current with its spectrum after compensation.
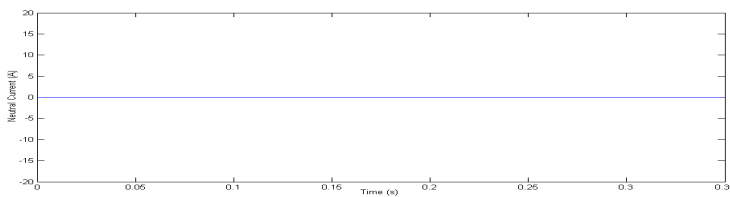

Fig. 8c. Neutral current after compensation.
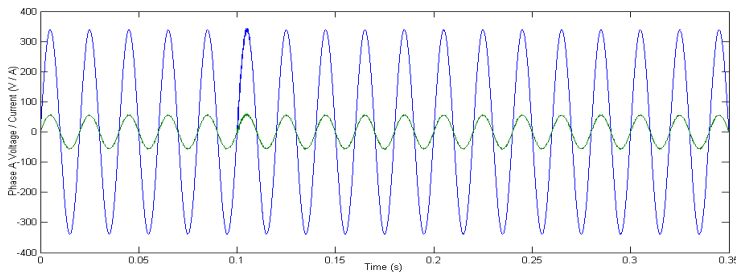

Fig. 8d. Source voltage and current of phase A after compensation.
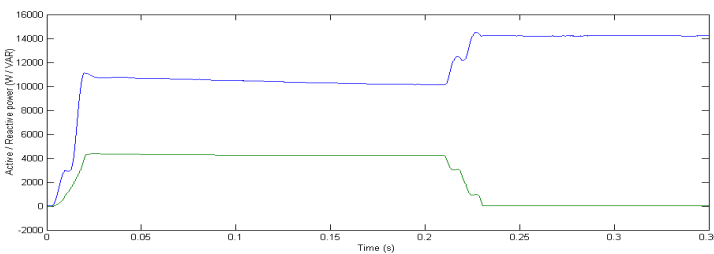

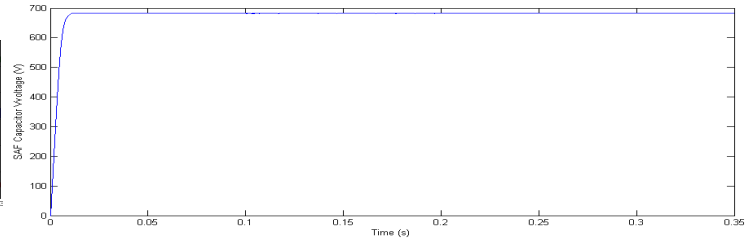**Fig. 9a**. Active and reactive power compensation.

Fig. 9b. Dc link capacitor voltage.

7. Conclusion

The performance of a new topology of three-phase four-wire SAF consisting of PV or battery operated boost converter fed Four-leg VSC with a T-connected transformer has been demonstrated for reactive power compensation, harmonic elimination, and neutral current compensation in interconnected utilities. The T-connected transformer improves the transient stability of a power system and also observed that its helps in damping low frequency power oscillations. The total kilovolt-amperes rating of the T-connected transformer is lower than the Zigzag-delta transformers and star-delta transformers for reactive power compensation and also it's found that harmonic mitigation techniques using T-connected transformer are a viable choice for mitigating rich triplen harmonics in four-wire electrical distribution system. T-connected transformer is also significantly reduced neutral current flowing back to the system almost up to 90%. A synchronous reference frame method has been presented for reactive power compensation, source harmonic reduction, and neutral current compensation. The boost converter is used to step up the voltage to match the dc link voltage of the four-leg VSC It is observed that the THD (Total Harmonic Distortion) of the source current for phase A is reduced from 20.80 to 1.48

Appendix A

AC line voltage	415 V, 50 Hz.
Line impedance	Rs = 0.01 Ω, Ls = 2mH.
Non-linear Three-phase bridge rectifier with R–L load	R = 25 Ω and L = 1 mH.

Ripple filter	Rf = 5 Ω, Cf = 5 µF.
Inductor	0.421 mH, 0.01 Ω.
DC bus capacitance	1500 µF.
DC bus voltage	680 V.
bus PI controller:	Kpq=1, Kiq=20.
PCC current PI controller:	Kpd = 1, Kid = 5.
PWM switching frequency	10 kHz.
T-connected Transformer	Two single-phase transformers Transformer 1: 2.5 kVA, 240V/120V/120V. Transformer 2: 2.5 kVA, 208V/208V.

REFERENCES

1] Mukhtiar Singh, Vinod Khadkikar, Ambrish Chandra, Rajiv K Varma, Grid Interconnection of renewable energy sources at the distribution level with power quality improvement features. IEEE Trans Power Deliver 2011; 26(1): 307–15.

[2] Ilango K, Bhargav.A Manjula G.Nair, Statcom interface for renewable energy sources with power quality improvement, Presented at the conference on power and energy system 2012; 2: 69-74.

[3] Chandani M. Chovatia, Prof. Narayan P. Gupta, Prof. Preeti N. Gupta, Power Quality Improvement in a PV Panel connected Grid System using Static Compensator, Inter J of Comp Tech and Elect Engg 2012; 2(4); 41-45

[4] T Jan, Bialasiewicz. Renewable energy systems with photovoltaic power generators: operation and modeling. IEEE Trans Indus Electronics 2008; 55(7): 2752–2758.

[5]A.Hari Prasad, Y.Rajasekhar Reddy. P.V. Kishore, Photovoltaic Cell as Power Quality conditioner for Grid connected system International Journal of Scientific & Engineering Research 2011; 2(10): 1-8

[6] IEEE Recommended Practices and Requirements for Harmonics Control in Electric Power Systems, IEEE Standard 519, 1992.

[7] S.K Khadem, M.Banu and M.F.Conlon, Power Quality in grid connected renewable energy systems: role of customer power devices. Presented at the conference IEEE renewable energy and power quality, spain; 2010.

[8] Bhim Singh, Kamal Al-Haddad, A Review of Active Filters for Power Quality Improvement, IEEE Transactions on industrial electronics,1999; 46(5):960-971

[9] D. Sreenivasarao, Pramod Agarwal, Biswarup Das, Neutral current compensation in three-phase, four-wire systems: A review,2012; 86: 170-180

[10] H. L. Jou, K. D. Wu, J. C. Wu, C. H. Li, and M. S. Huang, Novel power converter topology for three phase four-wire hybrid power filter, IET Power Electron.,2008; 1(1): 164–173.

[11] H. Fugita and H. Akagi, Voltage-regulation performance of a Static Compensator intended for installation on a power distribution system, IEEE Trans. Power Electron., 2007; 22(1): 1046–1053.

[12] Mehmet Ucar, Engin Ozdemir, Control of a 3-phase 4-leg active power filter under non-ideal mains voltage condition, Electric Power Systems Research, 2008; 78: 58–73

[13] Bhim Singh, P. Jayaprakash , D.P. Kothari, New control approach for capacitor supported DSTATCOM in three-phase four wire distribution system under non-ideal supply voltage conditions based on synchronous reference frame theory, Int J Electr Power Energy Syst 2011:33:1109-1117.Wind paper bang bang control

[14] S. Bhattacharya and D. Diwan, Synchronous frame based controller implementation for a hybrid series active filter system," in Proc. IEEE Ind. Appl. Soc. Meeting 1995, pp. 2531–2540.

[15] B. A. Cogbill and J. A. Hetrick, "Analysis of T–T connections of two single phase transformers," IEEE Trans. Power App. Syst., 1968; 87(2), 388–394.

[16] IEEE Guide for Applications of Transformer Connections in Three-Phase Distribution Systems, IEEE C57, R2008;.105-1978.

[17] B. Singh, V. Garg, and G. Bhuvaneswari, A novel T-connected autotransformer-based 18-

pulse AC–DC converter for harmonic mitigation in adjustable-speed induction-motor drives," IEEE Trans. Ind.Electron., 2007; 54(5): 2500–2511.

[18] R.Baker, G.Guth, W.Egli and P.Eglin, Control algorithm for a static phase shifting transformer to enhance transient and dynamic stability of large power systems, IEEE Trans., 1982; 101(9): 3532-3542.

[19] B. N. Singh, P. Rastgoufard, B. Singh, A. Chandra, and K. A. Haddad, Design, simulation and implementation of three pole/four pole topologies for active filters, in Inst. Electr. Eng. Proc. Electr. Power Appl., 2004; 151(4): 467–476.

[20] Tamil Nadu Agricultural Weather Network. <http://tawn.tnau.ac.in/>. <http://tawn.tnau.ac.in/action?action=lastMonthReport&block=49&district=6>.

[21]Photovoltaic modules data sheet. <http://www.planmypower.co.za>.

[22]http://solarpanels.greentechmedia.com/l/67/Canadian-Solar-CS5P-220Maspx>.

[23] Altas H, Sharaf AM. A photovoltaic array simulation model for MATLAB Simulink GUI environment. In: Proc ICCEP '07; 2007. p. 341–5.

[24] Park M, Yu In-K. A novel real-time simulation technique of photovoltaic generation systems using RTDS. IEEE Trans Energy Convers 2004; 19(1):164–9.

[25] Wei Jiang, Yu-fei Zhou, Jun-ning Chen. Modeling and simulation of boost converter in CCM and DCM. In: IEEE conference; 2009. p. 288–91.

[26] Mazouz N, Midoun A. Control of a DC/DC converter by fuzzy controller for a solar pumping system. Int J Electr Power Energy Syst 2011; 33(10):1623–30.

[27] S. Bhattacharya and D. Diwan, Synchronous frame based controller implementation for a hybrid series active filter system, in Proc. IEEE Ind. Appl. Soc. Meeting 1995, pp. 2531–2540.

[28] H. Kouara, H. Laib and A. Chaghi, A New Method to Extract Reference Currents for Shunt Active Power Filter in Three Phase Four Wire Systems, Int. Jour of Adv. Science & Technology, 2012; 46: 165-174.

[29] J. R. Hendershot and T. J. E. Miller, Design of Brushless Permanent Magnet Motors, Oxford, U.K.: Magna Physics, 1994.

[30] Vijayakumar, G & Karuppusamy, P 2017, Certain Investigation on Multilevel Inverters for Photovoltaic Grid Connected System, Journal of Circuits, Systems, and Computers, vol.25, no.9, pp. 1506 - 12.

[31] Vijayakumar, G, Karthikeyan, C & Ravi, V 2016, Operation of PV System With dc–dc Boost-Fed Shunt Active Filter (SAF)to Mitigate Current Harmonics and Energy Conservation', Journal of Testing and Evaluation, vol. 44, no. 1, pp. 342 -356.